

Topological crossovers near a quantum critical point

V. A. Khodel,^{1,2} J. W. Clark,² and M. V. Zverev^{1,3}

¹*Russian Research Centre Kurchatov Institute, Moscow, 123182, Russia*

²*McDonnell Center for the Space Sciences & Department of Physics,
Washington University, St. Louis, MO 63130, USA*

³*Moscow Institute of Physics and Technology, Moscow, 123098, Russia*

(Dated: January 20, 2013)

We study the temperature evolution of the single-particle spectrum $\epsilon(p)$ and quasiparticle momentum distribution $n(p)$ of homogeneous strongly correlated Fermi systems beyond a point where the necessary condition for stability of the Landau state is violated, and the Fermi surface becomes multi-connected by virtue of a topological crossover. Attention is focused on the different non-Fermi-liquid temperature regimes experienced by a phase exhibiting a single additional hole pocket compared with the conventional Landau state. A critical experiment is proposed to elucidate the origin of NFL behavior in dense films of liquid ^3He .

PACS numbers: 71.10.Hf, 71.10.Ay, 67.30.E-, 67.30.hr

The study of non-Fermi-liquid (NFL) behavior of strongly correlated Fermi systems in the regime of a quantum critical point (QCP) is currently one of the most active and challenging areas of condensed matter physics.^{1,2} As a rule, such behavior is attributed to second-order phase transitions, and the QCP is identified with the end point of a corresponding line of transition temperatures, denoted by $T_N(H)$ in the prototype in which an external magnetic field H is the control parameter. In this case, NFL behavior is triggered by critical antiferro- or ferromagnetic fluctuations, which lead to violation of respective Pomeranchuk stability conditions (PSC). Ensuing NFL phenomena are presumably explained either within the Hertz-Millis theory^{3,4} or, in heavy-fermion metals, within a Kondo breakdown model.^{1,2,5,6}

However, the widely promulgated fluctuation scenario is inconsistent with experimental data on a number of strongly correlated Fermi systems exhibiting NFL behavior:

- (i) In dense ^3He films where the emergent NFL behavior has been documented, experiment^{7–10} has not identified any related second-order phase transition.
- (ii) In several heavy-fermion metals^{11,12}, concurrent divergence of the Sommerfeld ratio $\gamma(T) = C(T)/T$ and the magnetic susceptibility $\chi(T)$ is observed at a point that is *separated by an intervening NFL phase* from termination points of any second-order phase transitions.
- (iii) In many instances of well-pronounced NFL behavior, the order parameters required to specify associated second-order phase transitions are still elusive, casting further doubt on the fluctuation scenarios.
- (iv) In external magnetic fields, thermodynamic properties demonstrate scaling behavior governed specifi-

cally by the ratio $\mu_f H/T$ where μ_f is the magnetic moment of constituent fermions.

These NFL phenomena can be understood when one recognizes that standard FL theory possesses its own quantum critical point, in the vicinity of which it fails. At this point, the *necessary* stability condition (NSC) for the $T = 0$ Landau state is violated,^{13–16} as opposed to violation of some PSC at a conventional QCP.

The NSC states that an arbitrary admissible variation $\delta n(p)$ from the FL quasiparticle momentum distribution $n_F(p) = \theta(p_F - p)$, while conserving particle number, must produce a positive change of the ground-state energy E_0 , i.e.,

$$\delta E_0 = \int \epsilon(p; n_F(p)) \delta n(p) dv > 0. \quad (1)$$

Here, $\epsilon(p; n_F)$ denotes the spectrum of single-particle excitations measured from the chemical potential $\mu(T=0)$ and evaluated for the initial Landau state specified by the quasiparticle occupancy $n_F(p)$. The reduction in energy due to breakdown of the NSC, which involves contributions linear in δn , is clearly larger than that due to violation of any PSC, which involves *bilinear* combinations of δn . We must conclude that any associated fluctuation scenario is irrelevant to the different type of QCP associated with violation of the NSC, which we shall call a Fermi-liquid QCP.

Violation of the NSC (1) is *unambiguously* linked to a change of the number of roots of equation

$$\epsilon(p, n_F) = 0. \quad (2)$$

In standard Fermi liquids, this equation has a single root at the Fermi momentum p_F , and in that case the signs of $\epsilon(p)$ and $\delta n(p)$ coincide, ensuring satisfaction of the NSC (1). However, consideration of the full Lifshitz phase diagram anticipates the emergence of additional roots of Eq. (2). For example, such roots appear at a critical density ρ_\diamond where the function $\epsilon(p, \rho_\diamond)$ attains either a

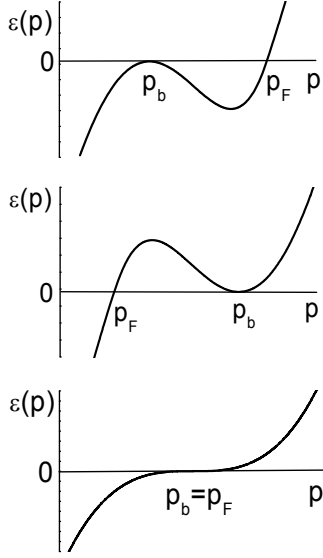


FIG. 1: Three scenarios of emergent bifurcation in Eq. (2): $p_b < p_F$ (top panel), $p_b > p_F$ (middle panel), $p_b = p_F$ (bottom panel).

maximum, with a bifurcation point $p_b < p_F$, or a minimum, with $p_b > p_F$, so that $\epsilon(p \rightarrow p_b, \rho_\infty) \propto (p - p_b)^2$, (see the upper two panels of Fig. 1). Thus, vanishing of $\epsilon(p_b, \rho_\infty)$ is always accompanied by vanishing of the group velocity $v(p_b, \rho_\infty) = (\partial\epsilon(p, \rho_\infty)/\partial p)_{p_b}$. Beyond the critical density ρ_∞ , the NSC fails to hold, since $\epsilon(p, n_F; \rho)$ and $\delta n(p)$ have opposite signs close to p_b .

As indicated in the lower panel of Fig. 1, the condition (1) is also violated at a critical density ρ_∞ where the effective mass $M^*(\rho)$ diverges. In this case, standard manipulations based on the Landau relation connecting the single-particle spectrum and the quasiparticle momentum distribution, (see Eq. (9) below) yield

$$\frac{v_F(\rho)}{v_F^0} \equiv \frac{M}{M^*(\rho)} = 1 - \frac{1}{3}F_1^0(\rho) \quad (3)$$

where $v_F^0 = p_F/M$ and $F_1^0(\rho) = f_1(p_F, p_F; \rho)p_F M/\pi^2$ is the dimensionless first harmonic of the Landau interaction function, normalized with the density of states $N_0 = p_F M/\pi^2$ of the ideal Fermi gas. Evidently, $F_1^0(\rho)$ is a smooth function of the density ρ , and $F_1^0(\rho) = 3$ at $\rho = \rho_\infty$. Then beyond the critical point, one has $F_1(\rho) > 3$, and the Fermi velocity $v_F(\rho)$ becomes negative. This behavior conflicts with the fluctuation scenario for the QCP, in which such a sign change is impossible.

To summarize, we infer that at any point where the NSC is violated, the density of states, given by

$$N(T) = \frac{1}{T} \int n(\epsilon)(1 - n(\epsilon)) \frac{dp}{d\epsilon} d\epsilon, \quad (4)$$

diverges at $T \rightarrow 0$ due to vanishing of the group velocity $d\epsilon(p)/dp$. One has^{15,17}

$$N(T \rightarrow 0, \rho_\infty) \propto T^{-2/3}, \quad N(T \rightarrow 0, \rho_\infty) \propto T^{-1/2}. \quad (5)$$

The difference in critical indexes is associated with the fact that $dp/d\epsilon \propto \epsilon^{-2/3}$ at the critical density ρ_∞ , whereas $dp/d\epsilon \propto |\epsilon|^{-1/2}$ at the critical density ρ_∞ .

Significantly, the Sommerfeld-Wilson ratio $R_{SW} = \chi(T)/\gamma(T)$ cannot diverge at these points. Indeed, the density of states $N(T)$ cancels out in the ratio R_{SW} , while the Stoner factor entering $\chi(T)$ maintains a finite value, since, as we have seen, the PSC and NSC cannot fail *at the same point*. This conclusion is in agreement with experimental data^{7,18,19} on dense films of liquid ^3He , the two-dimensional electron gas of MOSFETs, and the majority of heavy-fermion metals.

Since no symmetry is violated at a Fermi liquid QCP, and hence no hidden order parameters are involved, the transition ensuing from the violation of the NSC (1) is *topological* in character.^{20,21} Beyond the bifurcation point, Eq. (2) usually has two additional roots p_1 and p_2 situated near each other (however, cf. Refs. 22–24). It is for variations $\delta n(p)$ involving momenta $p_1 < p < p_2$, at which $\delta n(p)$ and $\epsilon(p)$ have opposite signs, that the NSC (1) breaks down.

The analysis of topological rearrangements triggered by the interaction between quasiparticles began twenty years ago,²² with important subsequent developments reported in Refs. 17,23–32. In this article, we address the Fermi-liquid QCP in homogeneous matter and focus on the case where the new roots p_1 and p_2 emerge near the Fermi momentum p_F . The physics of this phenomenon is captured if we keep the three first terms,

$$\begin{aligned} \epsilon(x) &= p_F x \left(v_F + \frac{v_1}{2}x + \frac{v_2}{6}x^2 \right), \\ v(x) &= v_F + v_1 x + \frac{v_2}{2}x^2, \end{aligned} \quad (6)$$

in the Taylor expansions of the spectrum $\epsilon(x)$ and its group velocity $v(x)$, where $x = (p - p_F)/p_F$. To some extent, this approach is reminiscent of that employed by Landau in his theory of second-order phase transitions. In an ideal Fermi gas, $v_F = v_1 = v_F^0 = (2M\epsilon_F^0)^{1/2}$. The case $v_1 = 0$, $v_2 > 0$ was considered in Ref. 17. Here we assume that $v_1 > 0$, $v_2 > 0$, and $v_1/v_2 \ll 1$, the situation addressed in the numerical calculations of Ref. 15.

To find the bifurcation momentum $p_b = p_F(1 + x_b)$ one must solve the set of equations $\epsilon(p) = 0$ and $v(p) = 0$, i.e.

$$\begin{aligned} v_F + \frac{v_1}{2}x_b + \frac{v_2}{6}x_b^2 &= 0, \\ v_F + v_1 x_b + \frac{v_2}{2}x_b^2 &= 0. \end{aligned} \quad (7)$$

This system has the solution $x_b = -3v_1/2v_2$ provided the critical condition

$$\frac{8v_2 v_F(\rho)}{3v_1^2} = 1 \quad (8)$$

is met. Thus in the case $v_1 \neq 0$, the critical Fermi velocity v_F is still *positive*, and therefore the Landau state becomes unstable *before* the system reaches the point at

which the effective mass diverges—as was first discovered and discussed in Refs. 25.

The prerequisite $x_b \ll 1$ for applicability of the expansion (6) is satisfied provided $v_1/v_2 \ll 1$, implying that the critical Fermi velocity is small: $v_F = 3v_1^2/8v_2 \ll v_F^0$. Given this situation, upon accounting for the dependence of v_F on the temperature T and control parameters such as the external magnetic field H that do not change the form of Eq. (8), one can establish a critical line $T = T_\diamond(H)$ separating phases with *different topological structure*.

Evaluation of relevant T - and H -dependent corrections to the Fermi velocity v_F is based on the Landau equation^{33,34} for the single-particle spectrum $\epsilon(p)$, which in 3D has the form

$$\frac{\partial \epsilon(p)}{\partial p} = \frac{p}{M} + \frac{1}{3} \int f_1(p, p_1) \frac{\partial n(p_1)}{\partial p_1} dv_1, \quad (9)$$

with $dv = p^2 dp/\pi^2$. This relation provides a nonlinear integral equation for self-consistent determination of $\epsilon(p, T, H)$ and the momentum distribution

$$n(p, T, H) = \left[1 + e^{\epsilon(p, T, H)/T} \right]^{-1}, \quad (10)$$

with the Landau interaction function $f(\mathbf{p}, \mathbf{p}_1)$ (hence its first harmonic f_1) treated as phenomenological input.

Our goal is to evaluate the T - and H -dependence of the key quantity $v_F(\rho, T, H)$. In the simplest case $H = 0$, the overwhelming T -dependent contributions to v_F come from integration over the vicinity of the bifurcation momentum p_b . Evaluation is performed along the same lines as in Ref. 17, i.e., by expanding the interaction function in a Taylor series, although here we have to retain a correction to the FL formula (3) linear in $p - p_b$. As a result, we arrive at

$$v_F(T \rightarrow T_\diamond) - v_F(\rho) \propto \int (s - p_b) \frac{\partial n(s, T)}{\partial s} ds, \quad (11)$$

where $v_F(\rho)$ is given by Eq. (3).

The integral I_T on the right side of Eq. (11) is evaluated with the aid of relations $\epsilon(p \rightarrow p_b) \propto (p - p_b)^2$ and $d\epsilon(p \rightarrow p_b)/dp \propto \sqrt{\epsilon(p)}$ stemming from Eq. (6). Upon standard changes of integration variables $p \rightarrow \epsilon \rightarrow Tz$, we find

$$I_T \propto T^{1/2} \int z^{1/2} n(z) (1 - n(z)) dz \propto \sqrt{T/\epsilon_F^0} \quad (12)$$

at $T \rightarrow T_\diamond$. Together with Eq. (8), this result leads to a tiny value of the critical temperature

$$T_\diamond \propto \epsilon_F^0 \left(\frac{v_1^2}{v_2 v_F^0} \right)^2 D^2, \quad (13)$$

where

$$D = 1 - 8 \frac{v_2 v_F^0}{3 v_1^2} \left(1 - \frac{1}{3} F_1^0(\rho) \right) \geq 0 \quad (14)$$

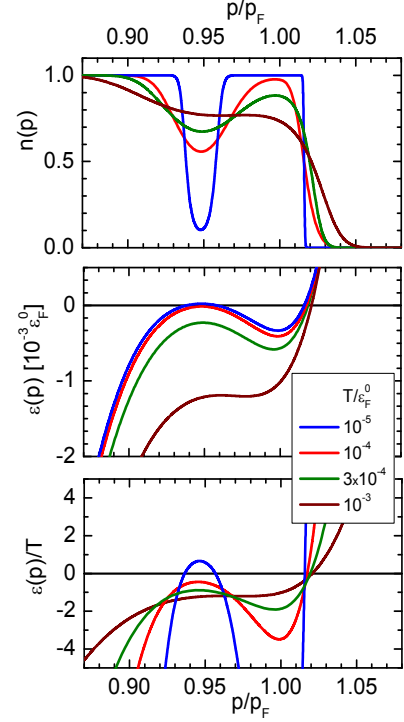


FIG. 2: Occupation numbers $n(p)$ (top panel), single-particle spectrum $\epsilon(p)$ in units of $10^{-3}\epsilon_F^0$ (middle panel), and ratio $\epsilon(p)/T$ (bottom panel) evaluated for the model (24) with $\kappa = 0.07$ and $g_s = 0.45$, at four color-coded temperatures (in units of ϵ_F^0) below $T_* = 3 \times 10^{-3}\epsilon_F^0$.

is a criticality parameter. Temperature T_\diamond vanishes at the point where $D = 0$.

Consider now the imposition of a magnetic field H on the system. The impact of the field becomes well pronounced when $\mu_f H > T$, and there emerge two subsystems having spin projections $\pm 1/2$, implying in turn a decomposition $N(T) = N_+(T) + N_-(T)$ of the density of states. The corresponding formulas are cumbersome and will be analyzed elsewhere. Here we focus on the case $T = 0$ and estimate an upper tuning magnetic field H_\diamond such that a bifurcation emerges in the spectrum $\epsilon_+(p)$, while the down-spin spectrum $\epsilon_-(p) = \epsilon_+(p) - 2\mu_f H$ admits merely the conventional root p_F^- . As before, a leading correction I_H to v_F comes from integration over the vicinity of the momentum p_b , with the subsystem whose spectrum goes to $\epsilon_+(p) \propto (p - p_b^+)^2 = Tz + \mu_f H_\diamond$ at $H \rightarrow H_\diamond$ making the dominant contribution, to yield

$$I_H \propto \int (Tz + \mu_f H_\diamond)^{1/2} n(z) (1 - n(z)) dz \propto \sqrt{\mu_f H_\diamond / \epsilon_F^0} \quad (15)$$

and

$$\mu_f H_\diamond \propto \epsilon_F^0 \left(\frac{v_1^2}{v_2 v_F^0} \right)^2 D^2. \quad (16)$$

Comparing Eqs. (13) and (16) we see that $\mu_f H_\diamond \sim T_\diamond$. This result is inherent to a scenario in which single-particle degrees of freedom play the dominant role and is consistent with available experimental data on heavy-fermion metals.^{19,35}

Let us now briefly analyze the situation at $T = H = 0$ on the ordered side of the topological rearrangement assuming, as before, the criticality parameter D to be positive. In the case $v_1 > 0$, addressed first in Refs. 25 and later in Ref. 15, the bifurcation momentum p_b resides inside the Fermi volume. The rearranged $T = 0$ quasiparticle momentum distribution $n(p)$ is given by $n(p) = 1$ for $p < p_1$ and $p_2 < p < p_F$, and zero otherwise, with p_F shifted outward to conserve quasiparticle number. Thus, the Fermi surface gains an additional hole pocket. In the 1960's, such a small hole pocket was called a Lifshitz bubble (LB) in Landau-school folklore. In this case, two additional roots of Eq. (2) appear, with

$$x_{1,2} = -\frac{3v_1}{2v_2} \left(1 \pm \sqrt{1 - 8 \frac{v_2 v_F(\rho; p_1, p_2)}{3v_1^2}} \right). \quad (17)$$

We note that $v_F(\rho, p_1, p_2)$ differs from the parameter $v_F(\rho)$ introduced previously, since it is evaluated for the phase in which the Fermi surface has three sheets. Accounting for the displacement of p_F due to emergence of the LB, one obtains $v_F(\rho, p_1, p_2) - v_F(\rho) \propto (p_1 - p_2)^2$, leading to

$$p_2 - p_1 \propto \frac{v_1}{v_2} \sqrt{D}. \quad (18)$$

As a result, we find

$$v_{LB} \propto \frac{v_1^2}{v_2} \sqrt{D} < v_F \quad (19)$$

for the LB Fermi velocity $v_{LB} = v(x_1)$ from the second of Eqs. (6), thereby demonstrating that the LB contribution to the density of states $N(0)$ prevails.

At temperatures beyond $T > T_\diamond$, the LB contribution to thermodynamic properties disappears. Were this to occur instantaneously, the specific heat $C(T)$ would undergo a jump, as if one were dealing with a second-order phase transition. As a matter of fact, the rearrangement occurs rapidly but not momentarily. Thus one deals with a *topological crossover* (TC), and Eqs. (7) serve to establish a TC line $T_\diamond(H)$ that resembles a line $T_N(H)$ of second-order phase transitions.

The TC width is found from the condition $T_< < T_\diamond < T_>$, with the boundaries $T_<$ and $T_>$ being determined by the relations

$$\epsilon(p_b, T_<) = T_\diamond, \quad \epsilon(p_b, T_>) = -T_\diamond. \quad (20)$$

Since $v(p, T) \simeq v_\diamond(p) \sqrt{T/\epsilon_F^0}$ in the LB region near T_\diamond , the similar formula $\epsilon(p, T) = (\epsilon_\diamond(p) - \epsilon_\diamond(p_F)) \sqrt{T}$ is obtained for the spectrum $\epsilon(p, T)$ after a simple momentum integration. Straightforward manipulations employing the definition $\epsilon(p_b, T_\diamond) = 0$ then lead to

$$\frac{T_> - T_\diamond}{T_\diamond} \simeq \frac{T_\diamond - T_<}{T_\diamond} \propto \sqrt{T_\diamond/\epsilon_F^0}. \quad (21)$$

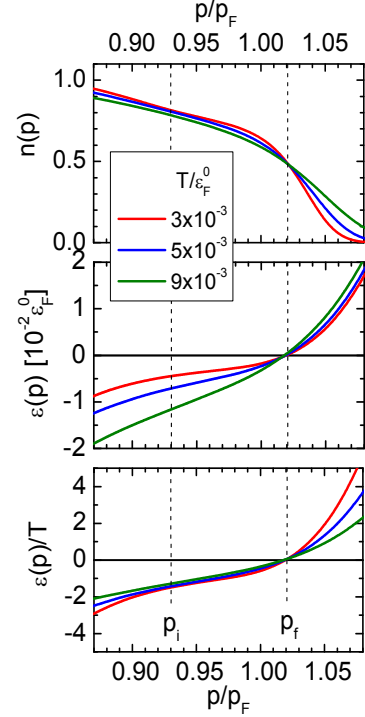


FIG. 3: Same as in Fig. 2 but at $T \geq T^*$.

Accordingly, the reduced temperature width of the critical region turns out to be small, implying that the TC does indeed imitate a second-order phase transition.

A conventional FL regime having T -independent quantities $\chi(0) \propto \gamma(0) \propto N(0) \propto 1/v_{LB}(0) \simeq 1/[v_F(0)\sqrt{D}]$ is seen to persist until T reaches $T_< < T_\diamond$, where the LB occupation numbers begin to experience substantial change as the temperature continues to increase. Both the density of states $N(T)$ and the spin susceptibility $\chi(T)$ attain maximum values at $T = T_\diamond$, where $\chi(T_\diamond) \propto 1/(v(x_b, T_\diamond)) \propto 1/\sqrt{T_\diamond}$. At higher temperatures, the LB contribution to $\chi(T)$ begins to fall, finally dying out and leaving $\chi(T) \propto 1/v_F(0)$. Analogous results are found for the Sommerfeld ratio, given by

$$\gamma(T) = \int \frac{\epsilon(p)}{T} \frac{\partial n(p)}{\partial T} dv, \quad (22)$$

except that γ reached its maximum at a different temperature, due to the marked dependence of the spectrum $\epsilon(p, T)$ on T . The foregoing analysis therefore leads to the conclusion that in the QCP region, both the magnetic susceptibility $\chi(T)$ and the Sommerfeld ratio $\gamma(T)$ exhibit *asymmetric peaks*, located at different temperatures $\simeq T_\diamond$. Such behavior, observed in many heavy-fermion metals situated in a QCP region,^{19,35,36} remains unexplained within any conventional scenario for the QCP.

Further temperature evolution of the spectrum $\epsilon(p, T)$ is associated with another essential rearrangement¹⁵ of the momentum distribution $n(p, T)$ that occurs in the

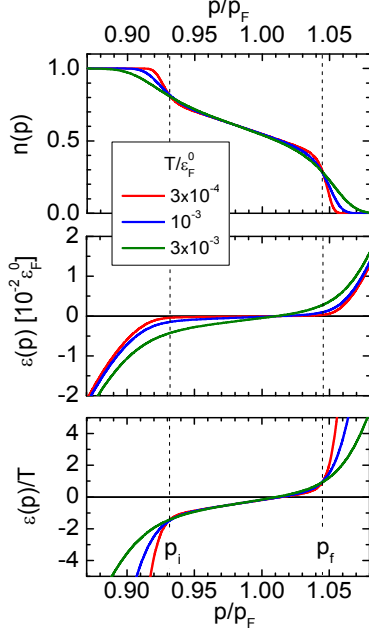


FIG. 4: Same as in Fig. 3 but for the interaction function (25) with the parameters $\alpha = 10$ and $g_y = 70$ at three line-type-coded temperatures.

region of a critical temperature T_* . The distribution $n(p, T)$ becomes a smooth function of momentum

$$n(p, T) \simeq n_*(p), \quad p_i < p < p_f, \quad (23)$$

in an interval adjacent to the Fermi surface and is otherwise unity for $p < p_i$ and zero for $p > p_f$. In this domain, $n(p, T)$ is nearly independent of T , while the dispersion of the single-particle spectrum $\epsilon(p, T)$ becomes proportional to T so as to satisfy Eq. (10).

Both these features are inherent to the phenomenon of fermion condensation, a *topological* phase transition discovered twenty years ago,^{13,22–24,37,38} in which a flat band pinned to the Fermi surface (the so-called fermion condensate (FC)) is formed. This phenomenon, alternatively viewed as a swelling of the Fermi surface, was recently rediscovered by Lee³⁹ while investigating the finite-charge-density sector of conformal field theory (CFT) within the AdS/CFT gravity/gauge duality. The phenomenon of fermion condensation (flat band) may also arise in topological media for purely topological reasons, (see Refs.40,41).

Unfortunately, important details of this rearrangement cannot be established analytically. To clarify the relationship between properties of the phase having the single LB at $T = 0$ and those of a system possessing a FC at $T = 0$, we must resort to numerical treatment of Eq. (9). Figs. 2 and 3 present results from numerical calculations¹⁵ of the spectra $\epsilon(p)$ and momentum distributions $n(p)$ for a 3D model system based on the inter-

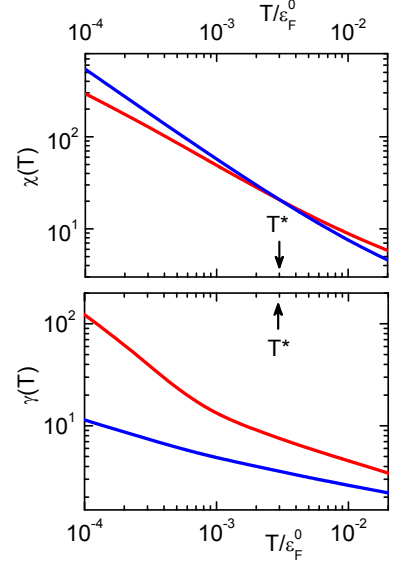


FIG. 5: Spin susceptibility $\chi(T)$ (top panel) and Sommerfeld ratio $\gamma(T) = C(T)/T$ (bottom panel), in Fermi gas units $p_F M/\pi^2$ and $p_F M/3$, respectively. Red curves show results for the model (24) and blue curves, for the model (25).

action function

$$f(q) = g_s \frac{\pi^2 p_F}{M} \frac{1}{q^2 + \beta^2 p_F^2} \quad (24)$$

with dimensionless parameters $g_s = 0.45$ and $\beta = 0.07$, values for which the zero- T phase possesses a single LB. In this model one has $T_\diamond \simeq 5 \times 10^{-5} \epsilon_F^0$ and $T_* = 3 \times 10^{-3} \epsilon_F^0$. The results are to be compared with those in Fig. 4 obtained for the model interaction function¹⁵

$$f(q) = g_y \frac{\pi^2}{M} \frac{e^{-\alpha q/p_F}}{q}, \quad (25)$$

for which a flat portion in the spectrum $\epsilon(p)$ is already present at $T = 0$. In the interval $T \simeq T_\diamond < T_*$, the spectra $\epsilon(p)$ of the two systems are quite dissimilar. However, when T reaches values around T_* , a flat portion of $\epsilon(p)$ develops for the interaction model (24) as well, the density associated with the flat segment being half the FC density ρ_* obtained for the model (25). On the other hand, outside the range $[p_i, p_f]$, the momentum distribution $n(p)$ calculated for model (24) shows more pronounced tails than in the case of model (25).

The impact of these differences on the magnetic susceptibilities χ and Sommerfeld ratios $\gamma(T)$ of the two model systems is seen in Fig. 5. As is known,^{42,43} the contribution χ_* of the FC region to χ obeys the Curie law: $\chi_*(T) \propto C_*/T$, with an effective Curie constant

$$C_* \propto \int n_*(p)(1 - n_*(p)) dv \propto \rho_*. \quad (26)$$

Fig. 5 shows that this Curie-like term does prevail in the susceptibilities calculated for both models. Such NFL

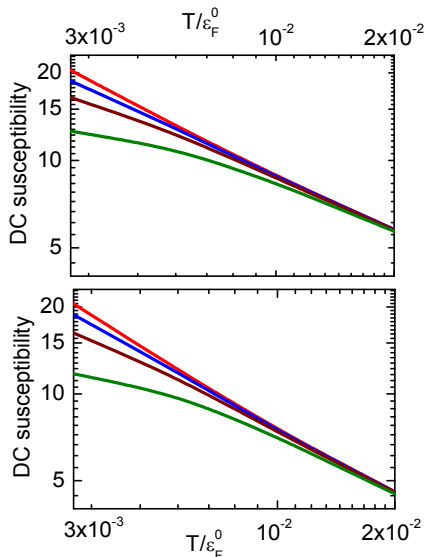


FIG. 6: DC susceptibility (in Fermi gas units) as a function of temperature (in units of ε_F^0) for different external-field magnitudes. Colors correspond to different values of $\mu_f H / \varepsilon_F^0$: 10^{-3} (red curve), 3×10^{-3} (blue curve), 5×10^{-3} (brown curve), 9×10^{-3} (green curve). Top panel: model (24), bottom panel: model (25).

behavior is in agreement with experimental data on dense films of liquid ^3He obtained in the QCP region.^{7,8,10}

The Sommerfeld ratios $R_{SW} = \chi(T)/\gamma(T)$ evaluated for the two models differ drastically. Indeed, in the LB case (i.e., for model (24)), the values of $\chi(T \rightarrow 0)$ and $\gamma(T \rightarrow 0)$ are large compared with those of the corresponding ideal Fermi gas, with R_{SW} remaining of order of unity. On the other hand, in the model (25) that already hosts a FC at $T = 0$, $\chi(T)$ diverges at $T \rightarrow 0$ as T^{-1} , while the FC contribution to $\gamma(T)$ evidently vanishes, implying a huge enhancement of R_{SW} . This scenario is in agreement with data⁴⁵ on the specific heat $C(T)$ of the P -type heavy-fermion metal YbIr_2Si_2 , for which the FL term $C(T) \propto T$ exists only at extremely low temperatures below T_\diamond , whose value is presumably less than 1 K. The corresponding value of $\gamma(T \rightarrow 0)$ is so enhanced that already at $T \simeq 0.7\text{K}$, the entropy value has become surprisingly large: $S/N \simeq (\ln 2)/2$. At $T > T_\diamond$ a collapse of $C(T)$ occurs, and the Landau term linear in T *completely disappears*. Thus, the P -type of the compound YbIr_2Si_2

presents the first example of a new class of metals, in which flattening of the single-particle spectrum results in an ordinary NFL shape of $C(T)$ at extremely low T .

Next, recall that in conventional Fermi liquids, the value of the susceptibility $\chi(T, H)$ is proportional to the density of states at finite field H , but is almost independent of H . By contrast, as witnessed in Fig. 6, an external magnetic field suppresses the NFL contribution to χ in Fermi systems whose spectra $\epsilon(p)$ exhibit a flat region (and to the same extent independent of which model is chosen). The larger the magnitude of the dimensionless parameter $\mu_f H / T$, the more pronounced is the suppression. These results, evaluated within the scheme elaborated in Refs. 17,31,44, elucidate the NFL behavior of dense liquid- ^3He films reported in Refs. 7–10. Taking for H a typical value of 1 T and for μ_f the magnitude of the ^3He atom's magnetic moment, the inequality $\mu_f H > T$ is met at $T < 0.5$ mK. Since temperatures below 0.2 mK are currently attainable, we suggest that it is experimentally feasible to verify or refute the predicted existence of a domain of the (T, H) phase diagram of 2D liquid ^3He sensitive to the magnitude of H .

We have investigated topological transitions arising in strongly correlated Fermi systems beyond a quantum critical point of the Fermi-liquid type, at which the density of states diverges while the Sommerfeld-Wilson ratio remains finite. We have attributed these transitions to violation of the *necessary* condition for stability of the Landau state. We have shown that in the QCP density region, the relevant phase diagram features different topological crossovers, occurring between states of the same symmetry but with different numbers of sheets of the Fermi surface. Importantly, the QCP scenario based on topological crossovers does not entail any order parameters; hence it is free from the persistent ambiguity of conventional fluctuation scenarios associated with hidden order parameters. Our analysis predicts the existence of a domain of the (T, H) phase diagram of 2D liquid ^3He that is sensitive to the magnitude of the magnetic field. This prediction is subject to experimental test.

The authors are grateful to E. Abrahams, H. Godfrin and V. Shaginyan for numerous helpful discussions. This research was supported by the McDonnell Center for the Space Sciences, by Grant Nos. 2.1.1/4540 and NS-7235.2010.2 from the Russian Ministry of Education and Science, and by Grant No. 09-02-01284 from the Russian Foundation for Basic Research.

¹ H. v. Löhneysen et al., Rev. Mod. Phys. **79**, 1015 (2007).

² P. Gegenwart, Q. Si, F. Steglich, Nature Phys. **4**, 186 (2008).

³ J. A. Hertz, Phys. Rev. B **14**, 1165 (1976).

⁴ A. J. Millis, Phys. Rev. B **48**, 7183 (1993).

⁵ Q. Si et al., Nature **403**, 804 (2001).

⁶ K. S. Kim, C. Pepin, Phys. Rev. B **81**, 205108 (2010).

⁷ K.-D. Morhard et al., J. Low Temp. **101**, 161 (1995); Phys. Rev. B **53**, 2568 (1996).

⁸ C. Bäuerle et al., J. Low Temp. **110**, 333 (1998).

⁹ A. Casey et al., Phys. Rev. Lett. **90**, 115301 (2003).

¹⁰ M. Neumann et al., Science **317**, 1356 (2007).

- ¹¹ S. L. Bud'ko, E. Morosan, P. C. Canfield, Phys. Rev. B **69**, 014415 (2004); **71**, 054408 (2005).
- ¹² J. Custers et al., Phys. Rev. Lett. **104**, 186402 (2010).
- ¹³ V. A. Khodel, V. R. Shaginyan, and V. V. Khodel, Phys. Rep. **249**, 1 (1994).
- ¹⁴ V. A. Khodel, JETP Lett. **86**, 721 (2007).
- ¹⁵ V. A. Khodel, J. W. Clark, and M. V. Zverev, Phys. Rev. B **78**, 075120 (2008); and references cited therein.
- ¹⁶ V. A. Khodel, J. W. Clark, and M. V. Zverev, JETP Lett. **90**, 628 (2009).
- ¹⁷ J. W. Clark, V. A. Khodel, and M. V. Zverev, Phys. Rev. B **71**, 012401 (2005).
- ¹⁸ V. T. Dolgoplov, Low Temp. Phys. **33**, 98 (2007).
- ¹⁹ P. Gegenwart et al., Acta Phys. Pol. **B 34**, 323 (2003).
- ²⁰ I. M. Lifshitz, Sov. Phys. JETP **11**, 1130 (1960).
- ²¹ G. E. Volovik, Springer Lecture Notes in Physics **718**, 31 (2007) [cond-mat/0601372]; and references cited therein.
- ²² V. A. Khodel and V. R. Shaginyan, JETP Lett. **51**, 553 (1990).
- ²³ G. E. Volovik, JETP Lett. **53**, 222 (1991).
- ²⁴ P. Nozières, J. Phys. I France **2**, 443 (1992).
- ²⁵ M. V. Zverev, M. Baldo, JETP **87**, 1129 (1998); J. Phys.: Condens. Matter **11**, 2059 (1999).
- ²⁶ S. A. Artamonov, V. R. Shaginyan, Yu. G. Pogorelov, JETP Lett. **68**, 942 (1998).
- ²⁷ M. V. Zverev, V. A. Khodel, M. Baldo, JETP Lett. **72**, 126 (2000).
- ²⁸ J. Quintanilla, A. J. Schofield, Phys. Rev. B **74**, 115126 (2006).
- ²⁹ N. Doiron-Leyrand et al., Nature **447**, 545 (2007).
- ³⁰ D. LeBoeuf et al., Nature **450**, 533 (2007); D. LeBoeuf et al., Phys. Rev. B **83**, 054506 (2011).
- ³¹ V. R. Shaginyan, JETP Letters **77**, 99 (2003); **79**, 344 (2004).
- ³² V. A. Khodel, P. Schuck, Zeit. Phys. **104**, 505 (1997).
- ³³ L. D. Landau, Zh. Eksp. Teor. Fiz. **30**, 1058 (1956).
- ³⁴ L. D. Landau and E. M. Lifshitz, *Course of Theoretical Physics*, Vol. 5, *Statistical Physics*, Third Edition (Nauka, Moscow, 1976; Addison-Wesley, Reading, MA, 1970).
- ³⁵ C. Krellner et al., Phys. Rev. Lett. **102**, 196402 (2009).
- ³⁶ C. Klingner et al., Phys. Rev. B **83**, 14405 (2011).
- ³⁷ V. R. Shaginyan, M. Ya. Amusia, and K. G. Popov, Phys. Usp. **50**, 563 (2007).
- ³⁸ V. R. Shaginyan et al., Phys. Rep. **492**, 31 (2010).
- ³⁹ S. S. Lee, Phys. Rev. D **79**, 086606 (2009).
- ⁴⁰ T. T. Heikilä, G. E. Volovik, JETP Lett. **93**, 59 (2011).
- ⁴¹ T. T. Heikilä, N. B. Kopnin, G. E. Volovik, arXiv:1012.0905.
- ⁴² M. V. Zverev and V. A. Khodel, JETP Lett. **79**, 635 (2004).
- ⁴³ V. A. Khodel, M. V. Zverev and V. M. Yakovenko, Phys. Rev. Lett. **95**, 236402 (2005).
- ⁴⁴ V. A. Khodel, P. Schuck and M. V. Zverev, Phys. Atomic Nuclei **66**, 1871 (2003).
- ⁴⁵ Z. Hossain, Phys. Rev. B **72**, 094411 (2005).